

## Interference of an array of atom lasers

Giovanni Cennini,<sup>1</sup> Carsten Geckeler,<sup>1,2</sup> Gunnar Ritt,<sup>1</sup> and Martin Weitz<sup>2</sup>

<sup>1</sup>*Physikalisches Institut der Universität Tübingen, Auf der Morgenstelle 14, 72076 Tübingen, Germany*

<sup>2</sup>*Institut für Angewandte Physik, Universität Bonn, Wegelerstr. 8, D-53115 Bonn*

(Received 11 July 2007; published 22 January 2008)

We report on the observation of interference of a series of atom lasers. A comblike array of atomic beams is generated by outcoupling atoms from distinct Bose-Einstein condensates confined in the different sites of a mesoscopic optical lattice. The observed interference signal arises from the spatial beating of the overlapped atom laser beams, which is monitored over a range corresponding to 2 ms of freefall time. The relative de Broglie frequencies and phases of the atom lasers were measured.

DOI: [10.1103/PhysRevA.77.013613](https://doi.org/10.1103/PhysRevA.77.013613)

PACS number(s): 03.75.Pp, 37.10.De, 37.25.+k, 37.10.Vz

Soon after the realization of optical lasers, the temporal interference signal among two such sources was observed [1]. This enabled investigations of the difference frequency and the frequency stability of the optical sources. To date, advances in the field of synthesizing and controlling optical frequencies allow for the measurement and comparison of optical frequencies with radio frequency precision [2,3]. Atom lasers are coherent atom sources whose outcoupled wave can be seen as a matter wave analog to the radiation emitted by optical lasers [4–8].

We report on an experiment observing the interference of an array of distinct atom laser beams. A series of rubidium atom clouds are initially cooled to quantum degeneracy in the sites of a mesoscopic optical lattice potential to form independent microcondensates. By smoothly ramping down the confining periodic potential, the condensates are coupled out into a comblike array of coherent, quasicontinuous atomic beams directed downwards along the earth's gravitational acceleration. Due to their divergence, the different atom laser beams soon overlap. The resulting interference pattern, as observed by absorption imaging, gives a streak-camera-like image of the beating of the coherent matter wave beams. The temporal evolution of the atom lasers relative phase was monitored over a vertical range corresponding to 2 ms of freefall time. The average difference frequency between adjacent atom laser sources was in a proof of principle experiment measured to an accuracy of 39 Hz.

Bose-Einstein condensates are coherent ensembles of particles, all populating a single one-particle state [10]. The coherence of such quantum degenerate samples has first been verified in interference experiments with two atomic Bose-Einstein condensates, leading to the conclusion that each condensate upon measurement can be described by a single, macroscopic quantum phase [11]. Recently, the relative phase of two Bose-Einstein condensates was continuously sampled by light scattering off the internal atomic structure [12]. On the other hand, light scattering can also imprint an atom phase [13]. Bose-Einstein condensated atoms can be outcoupled from their confining potentials to form atom laser beams [4–8]. By splitting up and recombining a single atom laser beam, its spectral linewidth was determined [14].

Our experiment is based on the technique of direct generation of Bose-Einstein condensates in optical dipole traps [8,15–17]. Initially, cold thermal rubidium atoms (<sup>87</sup>Rb) are

confined in the antinodes of a one-dimensional optical standing wave generated using midinfrared radiation derived from a CO<sub>2</sub> laser. Neighboring lattice sites are spaced by  $d = \lambda_{\text{CO}_2}/2 \approx 5.3 \mu\text{m}$ . By applying a magnetic field gradient of typically 10 G/cm, we remove atoms in magnetic field sensitive spin projections, yielding an ensemble of atoms all populating the  $m_F=0$  component of the lowest hyperfine ground state ( $F=1$ ). In each of the sites of the mesoscopic lattice, atoms are cooled evaporatively to quantum degeneracy. This produces an array of disk-shaped microcondensates, as described in more detail in [18]. Notably, due to the large spacing between sites the situation differs from work in near-resonant lattices, where tunnelling usually is non-negligible [19]. For our experimental parameters, the tunnelling time between adjacent sites during condensate preparation is so long that the condensates “have never seen each other” [9]. At the end of the evaporation stage, the CO<sub>2</sub> laser beam power is 40 mW on a 30  $\mu\text{m}$  beam radius. We generate an array of on average seven disk-shaped  $m_F=0$  microcondensates. The total number of atoms in this array is 2000. The atom laser beams are generated by, subsequently, in a 30-ms-long ramp, ramping the CO<sub>2</sub>-laser beam intensity towards zero smoothly. We nevertheless cannot exclude that small condensate excitations produced during this ramp can cause a small coupling between the different sources, which would lead to a correlation of the initial source phases. The outcoupling occurs once the dipole trapping force does not sustain the atoms against gravity anymore. In this way, a comblike structure of parallel atom laser beams directed downwards is produced. Due to the use of  $m_F=0$  condensates in our all-optical technique, fluctuations of the chemical potential due to stray magnetic fields are suppressed to within the 14 fK/(mG)<sup>2</sup> quadratic Zeeman shift of this (first-order) field-insensitive state [8].

We note that the spatial phase evolution of each atom laser is determined by the de Broglie wavelength  $\lambda = h/p$  with  $p^2/2m = \hbar\omega - mgz$ , where  $p$  is the momentum of atoms and  $h$  is the Planck's constant. One expects  $\lambda$  to decrease during the freefall as the momentum  $p$  increases. Despite this strong chirping of the spatial phase, monochromaticity of the matter waves is clearly defined [20–22]. In contrast, a time-dependent, fluctuating value of the chemical potential of the condensates would lead to deviations from merely gravitationally chirped matter waves, and relative variations can be

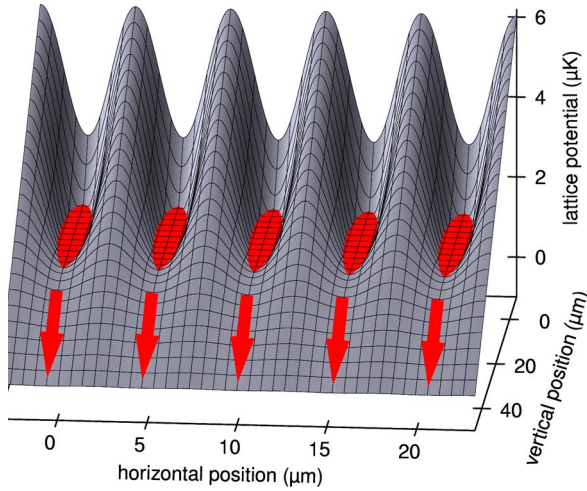


FIG. 1. (Color online) Scheme of the periodic trapping potential during the atom lasers emission. The emission occurs at the downwards directed surfaces of the microscopic traps, as indicated in the figure.

measured in interference experiments with other atom laser beams. More generally, such a comparison can also reveal other sources of differences in the beams frequency, such as variations in the vertical trap position, which will lead to a gravitational phase difference, or possibly even tiny differences in the atoms mass.

A scheme of the potential experienced by atoms during the onset of the atom laser beams operation is shown in Fig. 1. Before the condensates outcoupling, the trap vibrational frequencies are 1.9 kHz and 150 Hz along the longitudinal and the radial trapping directions of the lattice, respectively. The atom laser beams from adjacent sites are estimated to start overlapping at a time of 0.5 ms after outcoupling, and after 4 ms a complete overlap of all beams occurs.

We experimentally observe the far-field interference pattern of the atom lasers using absorption imaging. Figure 2(a)

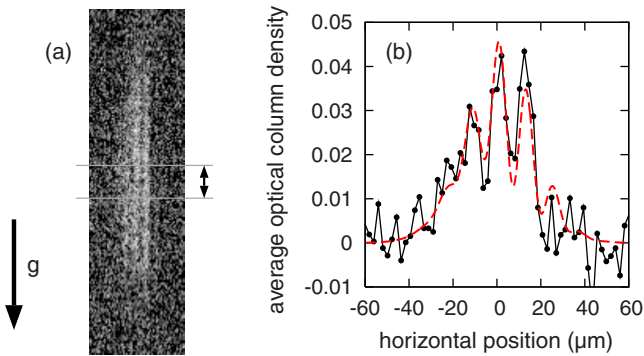


FIG. 2. (Color online) Far-field interference pattern of all-optical atom lasers. (a) Absorption image of the interference pattern of seven overlapped atom laser beams, recorded at an expansion time of 15 ms after the onset of outcoupling of atoms from the sites of the optical lattice. The field of view is  $60 \mu\text{m} \times 220 \mu\text{m}$ . (b) Horizontal density profile of image (a) averaged over the marked vertical region with  $44 \mu\text{m}$  height. The experimental data is represented by connected solid dots and the fitted fringe pattern by the dashed line.

shows a typical interference pattern for an average of seven populated sites in the lattice, which equals the number of interfering atom laser beams. The image gives a streak-camera-like recording of the interference pattern, in which the vertical position  $z$  relates to the fall time via the ballistic freefall formula. Figure 2(b) shows a transverse profile of the interference pattern averaged over a vertical length of  $44 \mu\text{m}$ .

Let us next discuss the expected interference signal for such an array of overlapping atom laser beams. We expect that the macroscopic wave function of each atom laser beam is given by an eigensolution of the Gross-Pitaevskii equation in the gravitational field. Due to the low density of the out-coupled atom beams far from the source, a single-particle Schrödinger equation can be used in the interference region. As the total number of atoms emitted from each source is fixed, we do not expect the atom lasers to have a well-defined phase. However, upon measurement of the interference pattern of the overlapping beams a projection upon a state with a well-defined relative phase is performed.

The optical lattice is in our experiment aligned orthogonally to the axis of gravity. Let us denote the macroscopic condensate wave function at the  $n$ th site ( $n = 1, 2, \dots, N$ ) centered at position  $\mathbf{r}_n$  at time  $t=0$  as  $a_n e^{i\theta_n}$ , where  $a_n$  gives the amplitude and  $\theta_n$  the phase. After outcoupling, the total wave function of the overlapping beams at position  $\mathbf{r}$  and time  $t$  (with  $t > 0$ ) can be formulated using path integrals evaluated along classical space-time trajectories [23] as follows:

$$\psi(\mathbf{r}, t) = \sum_{n=1}^N a_n e^{i\theta_n} C(\mathbf{p}, t_{\text{out}}) \exp \left[ \frac{i}{\hbar} \left( \int_{\mathbf{r}_{\text{trap},n}}^{\mathbf{r}} \mathbf{p} d\mathbf{r}' \right) - \int_0^t \hbar \omega_n dt' \right], \quad (1)$$

where  $\omega_n$  is the temporal de Broglie frequency of each atom laser defined as  $\hbar \omega_n = mgz_{\text{trap},n} + \mu_n(t')$ , and  $C(\mathbf{p}, t_{\text{out}})$  is a momentum-dependent function, which describes each atom laser envelope. This frequency is the sum of the initial atomic kinetic energy and  $n$ th condensates chemical potential  $\mu_n$ , where  $m$  denotes the atom mass and  $g$  the gravitational acceleration. We stress that the temporal phase fluctuations of both the initial condensates and the outcoupling process as well as fluctuations of the position of the confining laser beams are accounted for by assuming time-dependent chemical potentials  $\mu_n(t')$ . After outcoupling, due to energy conservation  $\hbar \omega_n$  remains constant, i.e.,  $\hbar \omega_n = mgz + \mu_n(t_{\text{out}})$  for  $t' > t_{\text{out}}$  (with  $0 \leq t_{\text{out}} \leq t$ ). We are interested in the total wave function outcoupled from the  $N$  sources all emitting at the same vertical position  $z_{\text{trap},n} = z_{\text{trap}}$ ,  $y_{\text{trap},n} = 0$ , and equally spaced along the  $x$  axis with  $x_{\text{trap},n} = dn$ , where  $d = \lambda_{\text{CO}_2}/2$  is the lattice spacing. After carrying out the above integrals, one can show that the probability to detect a particle at fixed time  $t$  and position  $\mathbf{r}$  in the far field can be written as

$$|\psi(\mathbf{r}, t)|^2 = |C(\mathbf{p}, t_{\text{out}})|^2 \sum_{n=1}^N A_n \cos \left[ \frac{ndm}{\hbar t_{\text{exp}}} x + \delta_n + \beta_n(z, t) \right], \quad (2)$$

where  $A_0 = \sum_{m=1}^N a_m^2$ ,  $\delta_0 = 0$  and for  $1 \leq n \leq N-1$ :  $A_n e^{i\delta_n} = 2 \sum_{m=1}^{N-n} a_m a_{m+n} e^{i\Delta\theta_m}$ . Both  $A_n$  and the phase angles  $\delta_n$  shall

here be real numbers. If the phase angles  $\Delta\theta_m = \theta_m - \theta_{m+n}$  are randomly distributed, as expected for truly independent sources, these coefficients can be evaluated in a random walk model with  $N-1$  steps [25]. If all amplitudes  $a_m$  are equal, for  $N \gg 1$  the average fringe visibility  $V \equiv A_1/A_0$  is then given by  $\sqrt{\pi/N}$ .

The  $z$ -dependent phase in Eq. (2) is

$$\beta_n(z, t) = \frac{1}{N-n} \sum_{m=1}^{N-n} [\varphi_m(z, t) - \varphi_{m+n}(z, t)] e^{i\Delta\theta_m}, \quad (3)$$

which again can be evaluated with a random walk model. In this formula  $\varphi_n(z, t) = (1/\hbar) \int_0^{t_{\text{out}}(z)} \mu_n(t') dt' + \mu_n(t_{\text{out}}(z)) [t - t_{\text{out}}(z)]$ . We expect that the mean square value of this  $z$ -dependent phase is approximately given by  $\sqrt{\langle \Delta\beta_n^2 \rangle} \approx \sqrt{\langle \Delta\varphi^2 \rangle}$ , which is independent of the number of condensates. Small statistical fluctuations of the chemical potential, which would lead to a line broadening, should affect the multiple beams interference pattern in a similar amount as in a two atom laser interference experiment. In case that the lattice axis is tilted against the axis of gravity by an angle  $\alpha$  (with  $\alpha \ll 1$ ), the cosine factor in Eq. (2) for  $|\psi|^2$  contains an additional factor  $\frac{nd}{\hbar} \alpha \sqrt{2m^2 g(z_{\text{trap}} - z)}$ , which in turn will lead to a tilting of the fringe pattern proportional to the lattice tilting.

The experimental interference pattern shown in Fig. 2 has high contrast (near 50%). With our present imaging resolution of  $6 \mu\text{m}$ , we spatially resolve only the interference pattern between adjacent lattice sites. Let us begin an analysis of the atom lasers interference pattern by restricting ourselves to signal profiles for a given fall distance  $|z - z_{\text{trap}}|$ , which corresponds to a fixed outcoupling time  $t_{\text{out}}$ . In this case, the amplitude and phase of the interference pattern are evaluated analogous to earlier work on the interference of independent Bose-Einstein condensates [18,24]. The fringe profiles were fitted with the function

$$I(x) = I_0 [e^{-(x-x_0)^2/\sigma^2} + V_{\text{exp}} e^{-(x-x_0')^2/\sigma'^2} \times \cos(2\pi x/\lambda_{\text{exp}} + \varphi_{\text{exp}})], \quad (4)$$

where  $\lambda_{\text{exp}}$ ,  $\varphi_{\text{exp}}$ , and  $V_{\text{exp}}$  denote the fitted fringe spacing, the phase angle of the interference pattern, and the fringe visibility of the pattern. Gaussian envelopes with independent widths and positions are here included for the background and fringe signals, respectively.

We have studied the variation of fringe contrast and phase angle for eight different realizations of the experiment. Figure 3 shows these parameters in a polar plot, where each dot corresponds to the result of an individual realization. A closer look at the plot reveals that most dots are located in the lower half, i.e., the phase angles are presumably not distributed randomly. In an earlier experiment on the interference of different condensates produced in our  $\text{CO}_2$ -laser lattice the observed random phase of the fringe signal gave clear evidence for the condensates being produced independently [18]. During the course of the outcoupling ramp of atom laser beams the potential barrier between different sites

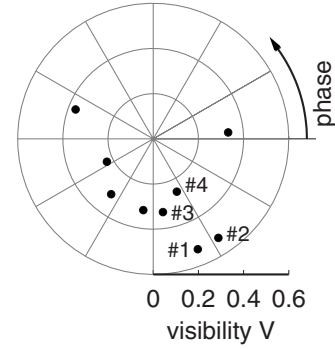


FIG. 3. The fringe visibilities and phase angles of fringe patterns arising from the interference of seven overlapped atom laser beams, as derived from fits as in Fig. 2(b), have been drawn (dots) in a polar diagram for eight different realizations of the experiment. The four measurements with the largest fringe were used to extract atom laser difference frequencies given in Table I.

is lower than during condensate preparation. However, for our experimental parameters the calculated single-atom tunneling time between adjacent sites for an atom in the condensate during both condensate preparation and any part of the outcoupling ramp is longer than  $10^{16}$  years due to the large spacing between sites. We are aware that collective condensate effects may decrease this tunneling time by a factor comparable to the order of the atom number, but this will still be much longer than our experimental cycle. The most likely explanation for the present observation seems to be a residual coupling of the source phase during the atom laser outcoupling process. During the now relatively slow ramping down of the optical potentials Fourier spectral components comparable to the vibrational frequencies arise, so that a residual coupling over the potential barriers between lattice sites due to condensate excitations could here occur. For the future, it is anticipated, that with different ramp speeds and ramp forms the coupling can be minimized. The average fringe contrast of the set of eight observed interference patterns with its corresponding standard deviation was  $(24 \pm 5) \%$ .

The present work involves atom lasers with (quasi-)continuous output coupling, and we can study the variation of the phase of the interference pattern with vertical position  $z$ , which directly is related to the duration of freefall. This allows us to monitor the atom lasers relative frequency. The vertical, stripelike nature of the fringes shown in Fig. 2 clearly shows that the temporal evolution of the atom laser phase over the observed 2 ms time window is well controlled. Fluctuations of the relative de Broglie frequencies here would lead to jittering or blurred fringes.

From Eq. (2) we expect that the fringe spacing increases linearly with the expansion time  $t_{\text{exp}}$  of atoms and is given by  $\hbar t_{\text{exp}}/(md)$ , where  $d$  is the spatial separation of sources. As the atoms during the outcoupling process already transversally expand before being completely removed from the trap potential, we set  $t_{\text{exp}} = t_{\text{fall}} + t_{\text{delay}}$  with  $z = z_{\text{trap}} - g t_{\text{fall}}^2/2$  describing the ballistic freefall and a constant term  $t_{\text{delay}}$  to account for the time lag during outcoupling in which atoms are not yet exposed to the earth's gravitational field alone. A fit to

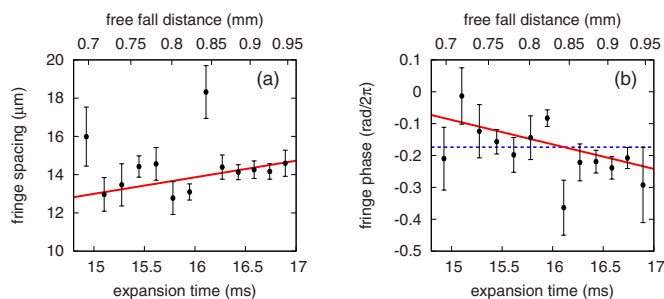


FIG. 4. (Color online) Fringe spacing and phase for the interference pattern of Fig. 2(a) as a function of the expansion time and of the corresponding freefall distance. (a) Experimental data for the fringe spacing evolution along with a linear fit (solid line). (b) Evolution of the fringe phase. The data has been fitted both with a constant (dashed line) and a linear function (solid line). The linear fit gives a finite slope which corresponds to an (average) difference frequency between adjacent atom lasers of  $-77$  Hz.

the experimental data for the pattern of Fig. 2 gives  $t_{\text{delay}} \approx 3$  ms, which is consistent with a simple numerical simulation. Figure 4(a) shows the experimental fringe spacing along with the fit (solid line) as a function of the expansion time.

Of particular interest is an analysis of the variation of the phase of the fringe pattern on the expansion time. The corresponding data is shown in Fig. 4(b). Over the observed 2 ms time interval, corresponding here to roughly  $250 \mu\text{m}$  of fall distance, the phase remains relatively constant with, on average, showing variations of an order of  $2\pi/10$ . The experimental data can both be fitted with a constant (dashed line) and linear (solid line) function of fall time, with the latter fit yielding a smaller sum of residuals. The nonzero slope of the latter fit translates to a finite difference frequency between adjacent atom lasers, as is, e.g., expected for a  $\text{CO}_2$ -laser lattice beam nonperfectly aligned orthogonal to the axis of gravity. Table I gives the fitted average atom laser difference frequency for this measurement (data set no.1) along with the result for three other high contrast fringe patterns. The average difference frequency between adjacent atom laser beams for the four data sets equals  $(-37 \pm 39)$  Hz. Notably, this result corresponds to the difference frequency of independently generated matter wave beams.

To conclude, we have observed the interference of an array of atom laser sources. The average relative phase fluctua-

TABLE I. Measured (averaged) difference frequency of neighboring atom laser beams. From a total of eight recorded interference patterns, with, due to the intrinsically random nature of the individual condensates phases, statistically distributed fringe contrast, these four sets had high enough contrast to allow for a reliable extraction of the average relative de Broglie frequency. We have fitted the measured differential phase with a linear function of the expansion time, as shown in Fig. 4(b) for data set no. 1. In the bottom row, the mean value for the matter wave frequency along with its standard deviation is given.

Data set number	$\delta\omega_{n,n-1}/\text{Hz}$
1	$-77 \pm 35$
2	$-75 \pm 44$
3	$-133 \pm 61$
4	$82 \pm 39$
Average	$-37 \pm 39$

tions and difference frequencies between adjacent matter wave sources were monitored. For the future, we expect that the relative measurement of atom laser frequencies can allow for novel matter wave metrology techniques.

An interesting question is, whether ultimately frequency measurements of small atomic mass differences can be carried out. An interference pattern between beams of different atomic species would be expected, if a mixing of mass eigenstates can be achieved, as could e.g., ultimately become possible with intense laser radiation given further advances in high power x-ray laser technology [26]. A second technical challenge for such an experiment clearly are the high values of the Schrödinger-de Broglie frequencies  $mc^2/\hbar$ , which for atoms are of the order  $10^{24}$ – $10^{25}$  Hz. X-ray laser radiation might simultaneously act as a local oscillator in a mass difference measurement, and in principle allow for frequency measurements of atomic mass differences in analogy to the neutrino oscillation experiments.

## ACKNOWLEDGMENTS

We acknowledge financial support from the Deutsche Forschungsgemeinschaft, the Landesstiftung Baden Württemberg, and the European Community.

- [1] A. Javan, E. A. Ballik, and W. L. Bond, *J. Opt. Soc. Am.* **52**, 96 (1962); T. S. Jaseja, A. Javan, and C. H. Townes, *Phys. Rev. Lett.* **10**, 165 (1963).
- [2] Th. Udem, R. Holzwarth, and T. W. Hänsch, *Nature (London)*, **416**, 233 (2003).
- [3] See, e.g., *Proceedings of the Sixth Symposium on Frequency Standards and Metrology*, edited by P. Gill (World Scientific, Singapore, 2002).
- [4] M.-O. Mewes, M. R. Andrews, D. M. Kurn, D. S. Durfee, C. G. Townsend, and W. Ketterle, *Phys. Rev. Lett.* **78**, 582 (1997).
- [5] B. P. Anderson and M. A. Kasevich, *Science* **282**, 1686 (1998).
- [6] I. Bloch, T. W. Hänsch, and T. Esslinger, *Phys. Rev. Lett.* **82**, 3008 (1999).
- [7] E. W. Hagley, L. Deng, M. Kozuma, J. Wen, K. Helmerson, S. L. Rolston, and W. D. Phillips, *Science* **283**, 1706 (1999).
- [8] G. Cennini, G. Ritt, C. Geckeler, and M. Weitz, *Phys. Rev. Lett.* **91**, 240408 (2003).
- [9] See, e.g., P. W. Anderson, in *The Lesson of Quantum Theory*,

- edited by J. de Boer, E. Dal, and O. Ulfbeck (Elsevier, Amsterdam, 1986).
- [10] E. A. Cornell and C. E. Wieman, *Rev. Mod. Phys.* **74**, 875 (2002); W. Ketterle, *ibid.* **74**, 1131 (2002).
- [11] M. R. Andrews, C. G. Townsend, H.-J. Miesner, D. S. Durfee, D. M. Kurn, and W. Ketterle, *Science* **275**, 637 (1997).
- [12] M. Saba, T. A. Pasquini, C. Sanner, Y. Shin, W. Ketterle, and D. E. Pritchard, *Science* **307**, 1945 (2005).
- [13] J. Denschlag, J. E. Simsarian, D. L. Feder, C. W. Clark, L. A. Collins, J. Cubizolles, L. Deng, E. W. Hagley, K. Helmerson, W. P. Reinhardt, S. L. Rolston, B. I. Schneider, and W. D. Phillips, *Science* **287**, 97 (2000).
- [14] M. Köhl, T. W. Hänsch, and T. Esslinger, *Phys. Rev. Lett.* **87**, 160404 (2001).
- [15] M. Barrett, J. Sauer, and M. S. Chapman, *Phys. Rev. Lett.* **87**, 010404 (2001).
- [16] S. R. Granade, M. E. Gehm, K. M. O'Hara, and J. E. Thomas, *Phys. Rev. Lett.* **88**, 120405 (2002).
- [17] T. Weber, J. Herbig, M. Mark, Hanns-Christoph Nägerl, and Rudolf Grimm, *Science* **299**, 232 (2003).
- [18] G. Cennini, C. Geckeler, G. Ritt, and M. Weitz, *Phys. Rev. A* **72**, 051601(R) (2005).
- [19] See, e.g., I. Bloch, *Phys. World* **17**, 25 (2004).
- [20] M. Holland, J. Burnett, C. Gardiner, J. I. Cirac, and P. Zoller, *Phys. Rev. A* **54**, R1757 (1996).
- [21] R. J. Ballagh, K. Burnett, and T. F. Scott, *Phys. Rev. Lett.* **78**, 1607 (1997).
- [22] For a different definition of the atom laser frequency, see H. M. Wiseman, *Phys. Rev. A* **56**, 2068 (1997).
- [23] R. Feynman and A. R. Hibbs, *Quantum Mechanics and Path Integrals* (McGraw-Hill, New York, 1965).
- [24] Z. Hadzibabic, S. Stock, B. Battelier, V. Bretin, and J. Dalibard, *Phys. Rev. Lett.* **93**, 180403 (2004).
- [25] S. Ashhab, *Phys. Rev. A* **71**, 063602 (2005).
- [26] See, e.g., T. Brabec and F. Krausz, *Rev. Mod. Phys.* **72**, 545 (2000).